

## Heavy-ion fusion at low energies

NEIL ROWLEY

Institut de Recherches Subatomiques, 23 rue du Loess, F67037 Strasbourg Cedex 2, France

**Abstract.** Through precision measurements of fusion cross sections at energies close to the Coulomb barrier and through the application of the method of “experimental barrier distributions” which these permit, many recent advances have been made in our understanding of the dynamical processes occurring during a heavy-ion collision. It is now clear that the target and projectile reach one another in superpositions of states which correspond to different orientations for rotational nuclei or to different induced deformations for vibrational nuclei. The creation of a neck of neutron matter has also long been postulated and by studying the isotopic dependence of the fusion reaction, some recent results in the  $^{40}\text{Ca} + ^{90,96}\text{Zr}$  systems appear to confirm this result. For large  $Z_1 Z_2$  a type of extra-push effect can arise from the same inelastic entrance-channel effects which enhance the fusion of lighter systems, though this will be absent in cases where the enhancement arises from neutron transfers.

The existence of different barriers will of course influence all other reaction channels. Fusion simply allows one to visualise the barriers most easily, since for this process, the total cross section is an *incoherent* sum of the contributions from all relevant eigenchannels. Some effects in other channels have already been observed. Other possible effects will be discussed. These include; the exploitation of the lowest-energy barrier to produce exotic evaporation residues and strongly deformed high-spin states at low excitation energy.

**Keywords.** Fusion barrier-distributions; exotic nuclei; deformed high-spin states.

**PACS Nos** 25.70.Jj; 25.70.Bc; 25.70.De; 25.70.Gh; 25.70.Hi; 21.60

### 1. Introduction

The fusion of two heavy-ions is not in itself a rare nuclear process, cross sections above the Coulomb barrier being of the order of the geometrical limit  $\pi R^2$  i.e. of the order of barns. However, many interesting phenomena do oblige us to study situations with much smaller cross sections, for example:

1) The dynamics of the entrance channel lead to a distribution of Coulomb barriers and a full understanding of this process can be obtained only by measuring the fusion cross section  $\sigma_f$  over a wide range of energies  $E$  both above and below the conventional barrier. If these data are sufficiently good, the ‘experimental barrier distribution’  $D(E)$  can be obtained from [1]:

$$D(E) = \frac{d^2(E\sigma_f)}{dE^2}. \quad (1)$$

2) The existence of barriers lowered in energy leads to the possibility of a small but significant compound-nucleus (CN) formation at lower excitation energies than one might

have expected, while still populating relatively high-spin states. The lower excitation energy may lead to reduced particle evaporation and thus to the formation of some relatively exotic nuclei which are not populated at higher  $E_{CN}^*$ .

3) It is well known that to form very heavy compound systems, in particular new elements, one is limited by the phenomenon of fission. The cross section for the formation of these high  $Z$  systems is the product of the fusion (passage to a compound nucleus) and the probability that they will survive fission. The latter probability increases with decreasing excitation energy and so taking advantage of entrance-channel effects may be of paramount importance here.

The first point outlined above i.e. the existence of a range of barriers, has been known for some time and over recent years the use of eq. (1) has given us significant insights into reaction dynamics. Figure 1 shows a representative selection of structures of fusion barriers which provide 'fingerprints' of different types of inelastic coupling which can intervene in sub-barrier fusion enhancement.

One sees in (1a) that for the system  $^{40}\text{Ca} + ^{40}\text{Ca}$  [2], where both target and projectile are

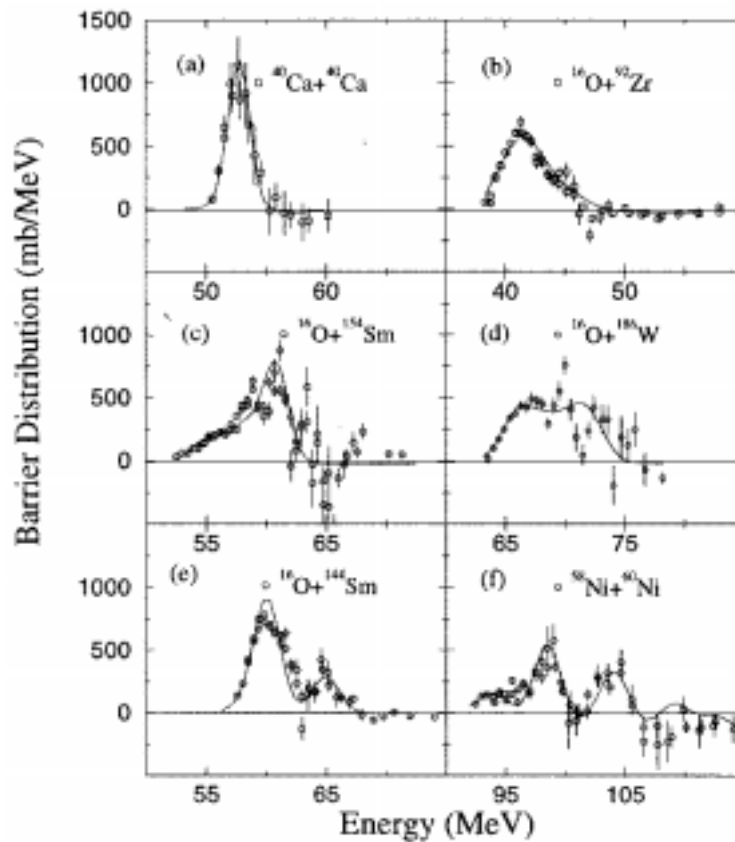


**Figure 1.** The great variety of experimental barriers distributions is demonstrated even when coupling is confined to inelastic excitations. Solid lines are theoretical results. See text.

double-closed-shell nuclei, a single peak is obtained with the width of around 3 MeV expected for a single Coulomb barrier. In (b), (c) and (d) essentially continuous distributions are seen. The latter two, corresponding to the spherical  $^{16}\text{O}$  on two different deformed systems [3,4], can be reproduced by summing the fusion from barriers corresponding to all possible orientations of the targets. However, the significant differences in  $D(E)$  can be related to a detail of the nuclear deformation; although  $^{154}\text{Sm}$  and  $^{186}\text{W}$  are both prolate rotors with large  $\beta_2$ , the former has a small positive hexadecapole moment whereas the latter has a small *negative*  $\beta_4$ . Frame (e) shows the double-peaked structure expected for strong coupling to a single-phonon state ( $3^-$  in  $^{144}\text{Sm}$ ) [5], while (f) shows a spectacular three-barrier structure due to complex surface vibrations induced by coupling to multiphonon states in the  $^{58}\text{Ni} + ^{60}\text{Ni}$  system [6]. In frame (b),  $^{16}\text{O} + ^{92}\text{Zr}$  [7] should display similar structures to the  $^{58}\text{Ni} + ^{60}\text{Ni}$  case. However, since the different Coulomb barriers correspond to variations of the nuclear radius, these effects scale as  $\beta Z_1 Z_2$ . The relatively low  $Z_1 Z_2$  value for this system causes the structures to overlap. They are thus 'unresolved' and the overall distribution appears continuous.

These experiments and many others have led to a deeper understanding of nuclear reaction mechanisms and shown quite unambiguously that the fusion cross section carries an enormous amount of information if only one looks carefully enough. Other results and consequences have been recently reviewed in detail in ref. [8].

In earlier studies of barrier distributions, Stelson and co-workers [9] claimed an important role for neutron transfer channels. However, for none of the above systems was it necessary to invoke such effects. Indeed for  $^{58}\text{Ni} + ^{60}\text{Ni}$ , it was expected that the elastic 2-neutron-transfer channel would have a strong effect but a comparison with an earlier experiment of Beckerman [10] showed that the structures for  $^{58}\text{Ni} + ^{58}\text{Ni}$  were practically identical to those in the present system. Since transfer  $Q$ -values are all rather different but the collectivity and excitation energies of the relevant phonon states are very similar, it was concluded that transfer played only a minor role.

Since it is clear that one cannot find systems where inelastic excitations do not come into play, it is necessary to look for isotopic effects in order to study neutron degrees of freedom. An ideal case would be a heavy double-closed-shell nucleus impinging on different isotopes of the same element (same  $Z_1 Z_2$ ), one having a closed neutron shell and the other having several neutrons outside the closed shell.

## 2. The $^{40}\text{Ca} + ^{90,96}\text{Zr}$ systems: Neutron necking

With the above considerations in mind, the  $^{40}\text{Ca} + ^{90,96}\text{Zr}$  systems were studied in detail at Legnaro [11]. The former target has a closed  $N = 50$  neutron shell, whereas the second has 6 neutrons outside that shell, all with positive  $Q$  values for transfer to the projectile.

Figure 2 compares the cross sections for these two systems. The dashed line shows the results of a calculation with no couplings to the  $^{90}\text{Zr}$  target. For the same system the solid curve shows that a good fit can be obtained by including inelastic excitations. Such a calculation fails, however, for the heavier target which has a further significant enhancement, apparently due to  $Q > 0$  neutron-transfer channels. Figure 3 shows the corresponding experimental barrier distributions and the fits arising from the calculations including inelastic excitations only. The failure to predict the low-energy barrier strength for  $^{96}\text{Zr}$  is manifest.

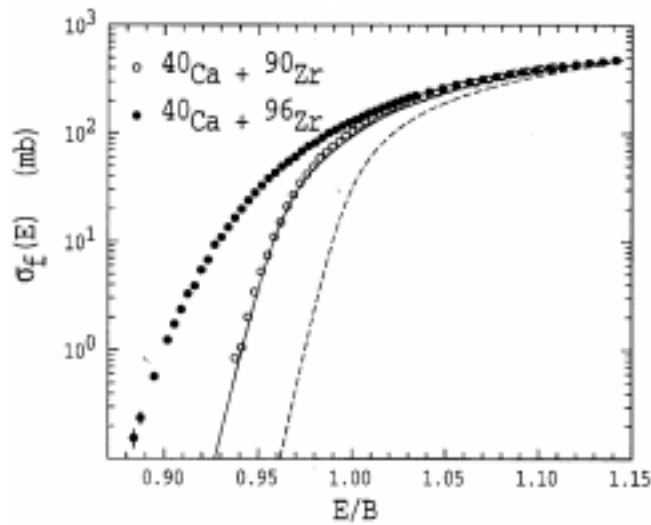


**Figure 2.** Fusion excitation functions for  $^{40}\text{Ca} + ^{90,96}\text{Zr}$  around the average barrier  $B$ . The dashed line shows the results of a calculation with no couplings for the former system. For the same reaction the solid curve shows that a good fit can be obtained by including inelastic excitations. Such a calculation fails for the latter case which has a further significant enhancement due to neutron-transfer channels. See text and figure 3.

An important consideration in fusing heavy systems is that at high  $Z_1 Z_2$ , Coulomb effects become more important. Of course the nuclear coupling is also proportional to  $Z_1 Z_2$  since it is determined by the changes in barrier height associated with changes in the nuclear radius. For systems with low excitation energy, where the initial configuration is essentially frozen, the relative importance of nuclear and Coulomb effects remains constant. However, for systems with high excitation energy, the long-range Coulomb interaction can polarise the nuclei well before the barrier is reached. Such a long-range polarization will always give a configuration unfavourable to fusion. These considerations are valid for inelastic excitations but of course for neutron-transfers, the Coulomb force has no effect. Thus the fusion of heavy systems might be facilitated by use of neutron-rich projectiles with many nucleons outside the closed shell available for transfer<sup>1</sup>.

### 3. Effects in other channels

The existence of different Coulomb barriers has been sought in other final channels with varying degrees of success. Both elastic [13] and quasi-elastic [14] channels do display

<sup>1</sup>Since this talk was presented, the possible creation of element  $Z = 114$  has been announced at Dubna [12]. The neutron excess of the  $^{48}\text{Ca}$  projectile used leads to a compound nucleus closer to the predicted island of stability but it is likely that it also plays the role discussed above of enhancing the fusion probability itself.

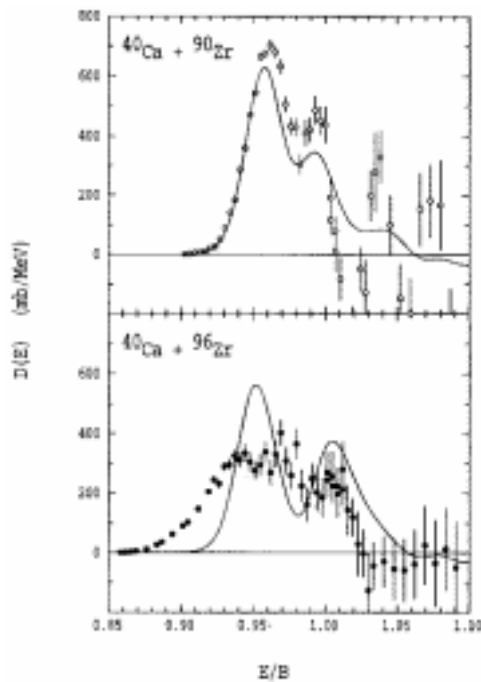


**Figure 3.** Experimental barrier distributions for  $^{40}\text{Ca} + ^{90,96}\text{Zr}$  along with the results of theoretical calculations including only inelastic excitations. These produce reasonable results for the former system but fail to give the low-energy strength in the latter case. Results are shown with respect to the corresponding average barrier  $B$ .

some evidence of the same gross structures observed in fusion (i.e. the overall width and shape of the distribution), however, the details of the individual peaks is often lost due to the fact that the relevant barrier amplitudes do not add incoherently thus giving rise to interference effects and dephasing.

Another important observation is that some dynamics of the fission channel may equally be related to entrance-channel effects, with the compactness of the formed compound nucleus depending on the orientation of a fusing deformed target, and leading to an energy-dependent fission anisotropy around the barrier region, which disagrees with the predictions of the statistical saddle-point method [15].

A recent experiment performed at the ANU [16] also suggests an important effect arising from the breakup channel. The system studied was  $^9\text{Be} + ^{208}\text{Pb}$ , which is of particular interest due to the *borromean* nature of the projectile. The results show what is effectively an overall renormalisation of the excitation function (hence the barrier distribution) due to the strong break-up channel.

An important consideration in fusion studies is how the different barriers may affect the properties of the compound nucleus formed i.e. how will the spin distribution be affected and will certain evaporation residues be favoured. We shall discuss these topics in the context of the  $^{58}\text{Ni} + ^{60}\text{Ni}$  system where additional experiments have been performed and are planned.

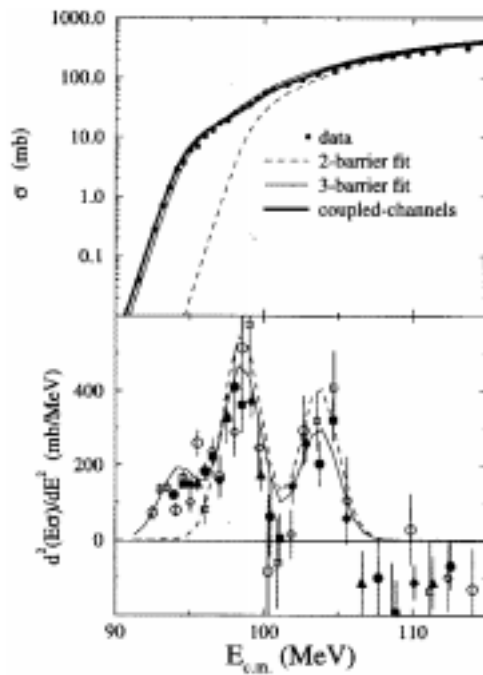


**Figure 4.** Experimental excitation function and barrier distribution for  $^{58}\text{Ni} + ^{60}\text{Ni}$ . The results of simple parametrized 2- and 3-barrier fits are shown along with the results of a full coupled-channels calculation.

#### 4. The $^{58}\text{Ni} + ^{60}\text{Ni}$ system: Feeding the compound nucleus

This reaction is of particular interest since the barrier distribution has three distinct peaks, as shown in more detail in figure 4. Reproducing this structure demands a rather full coupled-channels calculation, both from the point of view of which channels are included and how the dynamics are treated.

This is demonstrated in figures 5 and 6. Figure 5 shows the effects of the successive inclusion of higher-phonon channels. A good fit to the data is obtained only when one goes as far as the 4-phonon channel i.e. the double-mutual excitation of the quadrupole phonon vibrations in these nickel nuclei. Interestingly, the fit worsens if one supposes the existence of (unobserved) 3-phonon states in each nucleus, perhaps indicating a strong depletion of the collectivity as the single-particle space becomes blocked. This is an interesting example of a problem where the barrier fingerprint may give new information on the target and projectile internal structure.

Figure 6 shows the danger of approximations. A good fit is obtained only by taking account of couplings to all orders, finite excitation energies and Coulomb excitation at large  $r$ . This last effect suppresses the low-energy strength, increases the barrier centroid and, for high  $Z_1 Z_2$  may give rise to an effective extra-push energy.

The solid curves in figure 7 show the calculated spin distribution for the compound nucleus at three energies, each just above one of the three barriers of figure 4. The complex

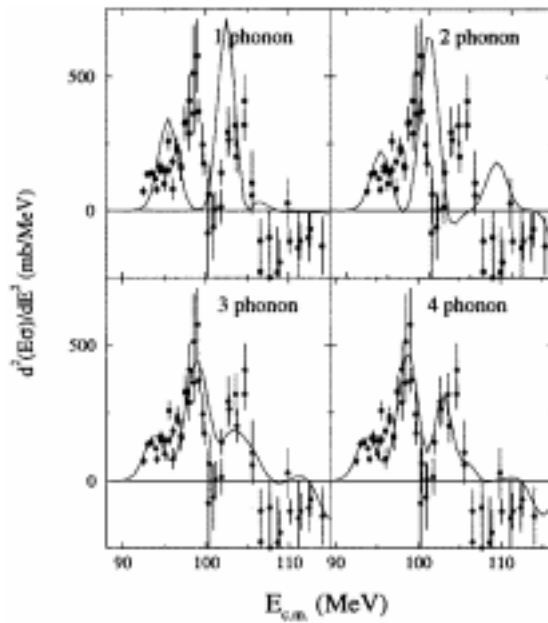


**Figure 5.** Results are shown for full coupled-channels calculations including from one to four phonons. In the one-phonon channel, the quadrupole phonon may be in either nucleus i.e.  $|1, 0\rangle$  or  $|0, 1\rangle$ . The four-phonon channel includes everything up to mutual-double excitation i.e.  $|2, 2\rangle$  but does not exceed two phonons in either nucleus.

structures are surprisingly simple to understand in terms of a smoothed triangular  $(2l + 1)$  distribution from each individual barrier, though the results shown emerge naturally from a full coupled-channels calculation. The great advantage of this system is that one can have considerable confidence in the predicted spin distributions since the same calculations fit a rather complex and highly enhanced fusion excitation function extremely well.

This was taken advantage of in a recent GAREL+ experiment at the Strasbourg Vivitron [17]. At each of the three energies, the discrete  $\gamma$ -ray transitions (near-yrast) were observed in order to see if the complexity of the initial distribution carried through to the yrast line. The rather remarkable result is that this is not the case, as shown by the data in figure 7. Indeed the shape of the spin population cuts off at around  $20\hbar$  for both the lower energies despite the much higher spin put into the compound nucleus. At the third energy a slight increase in  $\langle l \rangle$  is observed but nowhere near in proportion to the additional spin put into the compound nucleus.

This may be due to a relatively small spreading width  $\Gamma$  of states well above the yrast line at high spin, preventing the percolation down to the region of discrete decays. Such effects would of course strongly inhibit the population of super-deformed and hyper-deformed configurations at high spins. Thus understanding this phenomenon is of considerable importance. The fact that the flux starts to fall down rapidly at around spin  $20\hbar$ , may indicate a rapidly increasing  $\Gamma$  in this region and could be indicative of an order/chaos transition.

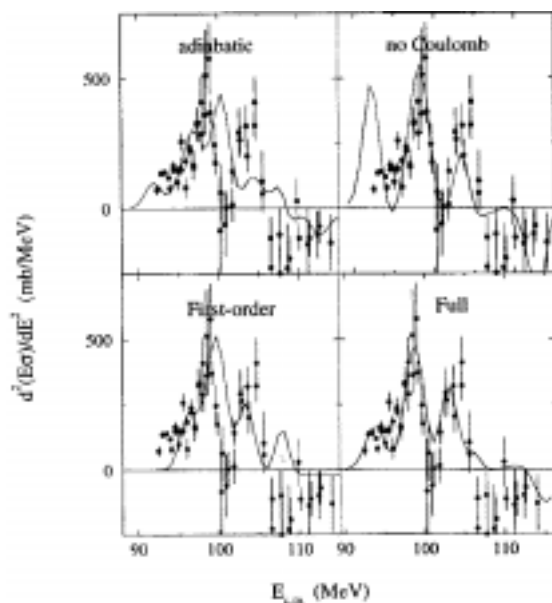


**Figure 6.** The four-phonon calculation of figure 5 is shown with various approximations: adiabatic (ignoring excitation energies), ignoring Coulomb excitation (note how Coulex suppresses the lowest barrier) and finally the effect of coupling only to first-order.

Other interesting features arising from the lowest barrier are:

- 1) The compound nucleus formed by fusion through the lowest barrier is created with a large prolate deformation due to the initial distortion of the target and projectile. If this shape survives sufficiently long, it should lead to enhanced charged-particle emission. Indeed a significant enhancement of proton emission, relative to evaporation-code predictions, is observed at the lowest energy [17].
- 2) The possibility of fusion at energies below the conventional Coulomb barrier could lead to the survival of some exotic neutron-deficient nuclei. Indeed at the lowest energy,  $^{116}\text{Cs}$  is predicted. This nucleus is 17 neutrons away from  $\beta$ -stability and lies very close to the proton-drip line. It has no known  $\gamma$ -rays.

The  $^{58}\text{Ni} + ^{60}\text{Ni}$  experiment will be repeated at Legnaro using GASP and the recoil mass spectrometer. The GASP inner ball will allow us to extract the total  $\gamma$ -ray spin distribution i.e. that prevailing after particle evaporation. This will give greater insight into where the entrance-channel angular momentum is lost and will also provide invaluable information for the calculation of the ensuing continuum  $\gamma$ -decays, thus enabling a better evaluation of the spreading width  $\Gamma$ . The use of the RMS will also allow a gating on  $^{116}\text{Cs}$  to test whether one can exploit entrance-channel effects to populate very proton-rich nuclei at relatively high spins.

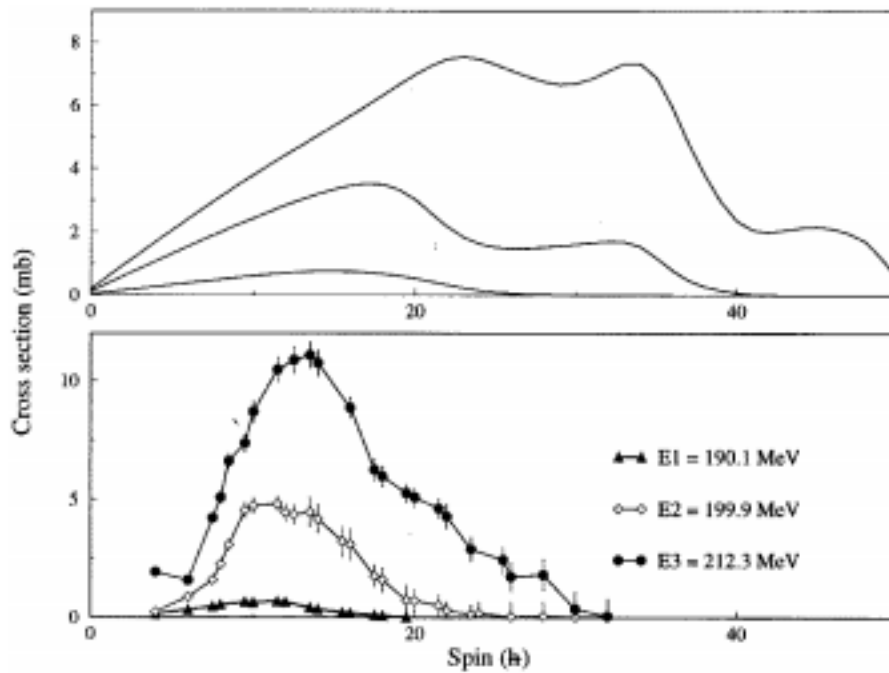


**Figure 7.** The angular momentum of the compound nucleus at formation is compared with the measured spin distribution for near-yrast (discrete)  $\gamma$ -decays at various energies.

## 5. Conclusions

The extraction of a fusion barrier distribution from experimental data is now very well established, as are many of its experimental consequences [8]. The demands for good statistics are well rewarded by the ensuing information which frequently gives enormous insights into nuclear reaction dynamics and presents a real challenge to theoretical analysis.

We have already seen the reflection of these barriers in other reaction channels; elastic, inelastic and even fission and are beginning to learn how to exploit their influence on the formation of the compound nucleus both in the spin and isospin degrees of freedom, and possibly ultimately in the creation of systems of higher mass and charge. Of course studies of fusion with radioactive beams have also started (see e.g. refs [18,19]) and we also look forward to many interesting new results in that domain.

## References

- [1] N Rowley, G R Satchler and P H Stelson, *Phys. Lett.* **B254**, 25 (1991)
- [2] H A Aljuwair *et al*, *Phys. Rev.* **C30**, 1223 (1984)
- [3] J X Wei, J R Leigh, D J Hinde, J O Newton, R C Lemmon, S Elfström, J X Chen and N Rowley, *Phys. Rev. Lett.* **67**, 3368 (1991)

- J R Leigh, N Rowley, R C Lemmon, D J Hinde, J O Newton, J X Wei, J Mein, C R Morton, S Kuyucak and A T Kruppa, *Phys. Rev.* **C47**, R437 (1993)
- [4] R C Lemmon, J R Leigh, J X Wei, C R Morton, D J Hinde, J O Newton, J C Mein, M Dasgupta and N Rowley, *Phys. Lett.* **B316**, 32 (1993)
- [5] C R Morton, M Dasgupta, D J Hinde, J R Leigh, R C Lemmon, J P Lestone, J C Mein, J O Newton, H Timmers, N Rowley and A T Kruppa, *Phys. Rev. Lett.* **72**, 4074 (1994)
- [6] A M Stefanini, D Ackermann, L Corradi, D R Napoli, C Petrache, P Spolaore, P Bednarczyk, H Q Zhang, S Beghini, G Montagnoli, L Mueller, F Scarlassara, G F Segato, F Sorame and N Rowley, *Phys. Rev. Lett.* **74**, 864 (1995)
- [7] J C Mein *et al*, private communication
- [8] M Dasgupta, D J Hinde, N Rowley and A M Stefanini, *Ann. Rev. Nucl. Part. Sci.* **48**, 401 (1998)
- [9] P H Stelson, H J Kim, M Beckerman, D Shapira, and R L Robinson, *Phys. Rev.* **C41**, 1584 (1990)
- [10] M Beckerman *et al*, *Phys. Rev. Lett.* **45**, 1472 (1980); *Phys. Rev.* **C23**, 1581 (1981)
- [11] H Timmers, L Corradi, A M Stefanini, D Ackermann, J H He, S Beghini, G Montagnoli, F Scarlassara, G F Segato and N Rowley, *Phys. Lett.* **B399**, 35–39 (1997)
- H Timmers, D Ackermann, S Beghini, L Corradi, J H He, G Montagnoli, F Scarlassara, A M Stefanini and N Rowley, *Nucl. Phys.* **A633**, 421–445 (1998)
- [12] “Element 114 lumbers into view”; *Science* **283**, 474 (1999)
- [13] N Rowley, H Timmers, J R Leigh, M Dasgupta, D J Hinde, J C Mein, C R Morton and J O Newton, *Phys. Lett.* **B373**, 23–29 (1996)
- [14] H Timmers, J R Leigh, M Dasgupta, D J Hinde, R C Lemmon, J C Mein, C R Morton, J O Newton and N Rowley, *Nucl. Phys.* **A584**, 190 (1995)
- [15] D J Hinde, M Dasgupta, J R Mein, J C Morton, J O Newton and H Timmers, *Phys. Rev.* **C53**, 1290 (1996)
- [16] M Dasgupta *et al*, *Phys. Rev. Lett.* **82**, 1395 (1999) and contribution to this conference
- [17] S Courtin *et al*, in progress
- [18] V Fekou-Youmbi *et al*, *Nucl. Phys.* **A583**, 811 (1995)
- [19] A Yoshida *et al*, *Nucl. Phys.* **A588**, 109c (1995)